ACS APPLIED MATERIALS & INTERFACES

Research Article

www.acsami.org

More Dominant Shear Flow Effect Assisted by Added Carbon Nanotubes on Crystallization Kinetics of Isotactic Polypropylene in Nanocomposites

Junyang Wang,[†] Jingjing Yang,[†] Liang Deng,[†] Huagao Fang,[‡] Yaqiong Zhang,[†] and Zhigang Wang*[,†]

[†]CAS Key Laboratory of Soft Matter Chemistry, Department of Polymer Science and Engineering, Hefei National Laboratory for Physical Sciences at the Microscale, University of Science and Technology of China, Hefei, Anhui Province 230026, P. R. China

[‡]Provincial Key Laboratory of Advanced Functional Materials and Devices, Institute of Polymer Materials and Chemical Engineering, School of Chemistry and Chemical Engineering, Hefei University of Technology, Hefei, Anhui Province 230009, P. R. China

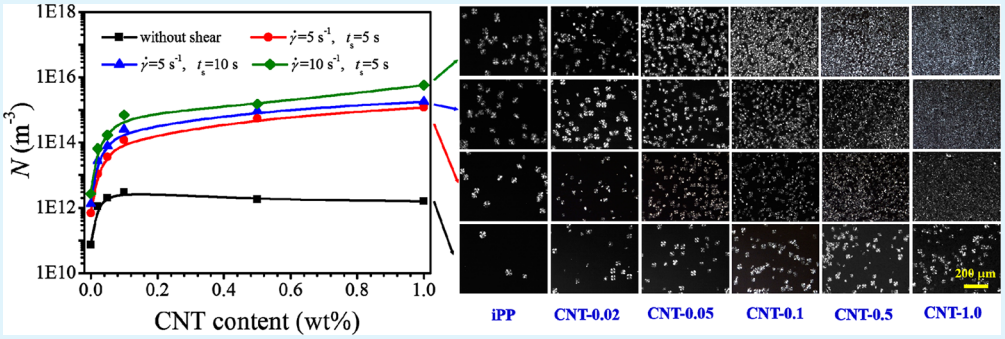

ABSTRACT: More dominant shear flow effect with different shear rates and shear time with assistance of added carbon nanotubes (CNTs) of low amounts on the crystallization kinetics of isotactic polypropylene (iPP) in CNT/iPP nanocomposites was investigated by applying differential scanning calorimetry (DSC), polarized optical microscopy (POM), and rheometer. CNTs were chemically modified to improve the dispersity in the iPP matrix. CNT/iPP nanocomposites with different CNT contents were prepared by solution blending method. The crystallization kinetics for CNT/iPP nanocomposites under the quiescent condition studied by DSC indicates that the addition of CNTs of low amounts significantly accelerates crystallization of iPP due to heterogeneous nucleating effect of CNTs, whereas a saturation effect exists at above a critical CNT content. The shear-induced crystallization behaviors for CNT/iPP nanocomposites studied by POM and rheometry demonstrate the continuously accelerated crystallization kinetics with assistance from added CNTs, with increasing CNT content, shear rate, and shear time, without any saturation effect. The changes of nucleation density for CNT/iPP nanocomposites under different shear conditions can be quantified by using a space-filling modeling from the rheological measurements, and the results illustrate that the combined effects of added CNTs and shear flow on the acceleration of crystallization kinetics are not additive, but synergetic. The mechanisms for the synergetic effect of added CNTs and shear flow are provided.

KEYWORDS: *shear-induced crystallization, nucleation density, spherulitic growth rate, rheology*

INTRODUCTION

Carbon nanotubes (CNTs), which possess small dimensions, low density, large aspect ratio, high mechanical strength, and high electrical conductivity, have attracted great attention in physics, chemistry, materials, and other research areas.[1] Among all the applications of CNTs, CNT/polymer composites represent one of the most favorable commercial applications.[2,3] Researchers have concentrated on studies of mechanical[4,5] and electrical properties,[2,6] thermal stability, and flame retardancy of CNT/polymer composites for obtaining the materials with excellent applicable properties. On the other hand, the final properties of most semicrystalline polymers depend on the microstructures, which are mainly affected by crystallization.[7] Addition of CNTs into semicrystalline polymers can profoundly change the crystallization kinetics and morphologies, such as increases in nucleation density and crystallization rate, and decrease in crystalline phase scale.[8−13] By providing heterogeneous nucleation sites, CNTs can reduce the nucleation energy barrier for polymer crystallization,[14−16] and it has been widely accepted that the macromolecular chain segments are able to be absorbed onto the CNT surface and become locally aligned, which subsequently induce nucleation and template the crystal growth.[17]

For polymer processing (e.g., injection molding, extrusion, and film blowing), the polymer composites are inevitably subjected to shear flow, which can enhance the crystallization kinetics.[18] The typical "shish-kebab" morphology, which can improve the ultimate mechanical properties of shaped products,

Received: November 12, 2014
Accepted: December 23, 2014
Published: January 8, 2015

DOI: 10.1021/am507938s
ACS Appl. Mater. Interfaces 2015, 7, 1364−1375

is usually induced by shear flow through stretching of the high molecular mass chains and the subsequent formation of shish structure, onto which the shorter chains grow epitaxially to form the kebabs.[19,20] The crystallization kinetics for CNT/polymer composites under shear flow might be quite different, because CNTs can assist in the formation of extended polymer chain fibrils to generate the hybrid shish and disk-shaped polymer crystals (kebabs) growing epitaxially onto the hybrid shish, resulting in the nano-hybrid shish-kebabs (NHSK) morphology.[21−23] It has been confirmed that the nanohybrid shish forms with an oriented layer of aligned macromolecular chains, induced by the coeffects of CNTs and shear flow, indicating that CNTs play an important role in the formation of oriented nuclei, especially at the shear flow conditions where the oriented nuclei cannot form in the absence of CNTs.[24] The enhancement effect on shear-induced crystallization by addition of CNTs cannot be simply attributed to their heterogeneous nucleation ability, because the CNTs embedded in the polymer melt under shear flow restrain the relaxation of the long-range motion of macromolecular chains by the surface absorption effect.[25−29]

The characteristics of the added CNTs in polymer composites, such as sizes, shape, and content affect the final crystalline structures and morphologies.[30] However, when shear flow is applied, the influences tend to depend on shear rate, shear time, and the coupling between shear flow and CNT characteristics.[31−36] Because the coexistence of additives and shear flow makes the crystallization process much more complicated, the effects of both factors on the crystallization kinetics of polymer composites have not been studied extensively and meticulously so far. D'Haese et al.[36,37] studied systematically the combined effects of particles and shear flow on the crystallization of polymers and concluded that at the shear flow condition with low shear rates, heterogeneous nucleation by particles accelerates the crystallization kinetics; however, at sufficiently high shear rates, shear flow will dominate the nucleation, and the crystallization kinetics is found to be independent of the particles characteristics. This conclusion, together with the results from Naudy et al.,[38] suggests an additive rule of the effects of particles and shear flow on polymer crystallization kinetics. As for CNT/polymer composites, although a synergetic effect rather than an additive rule of the presences of CNTs and shear flow on the promotion of crystallization kinetics has been pointed out and authenticated,[10,11,39] the contributions of either added CNTs or shear flow to the total synergetic effect have not been evaluated for revealing which one plays a more prominent role in this type of synergetic effect. From the conventional crystallization viewpoint, the crystallization kinetics includes two aspects, the nucleation and crystal growth, which leaves us another fundamental question, for which aspect the synergetic effect of added CNTs and shear flow mainly plays.

Recently, with the ability of simulating the polymer processing conditions, rheometry has been applied to investigate the shear-induced crystallization for various polymers.[18,25,40−43] Through modeling the crystallization process, important information such as the evolutions of crystalline morphology, crystallization half-time, degree of space-filling, and nucleation density can be obtained easily and even more accurately than some other traditional methods.[40,42,44] Regarding the determination of the nucleation density, rheological measurement has some important advantages; that is, it is applicable to the systems where optical microscopy does not work, and it is much easier, faster, and more accurate than the optical methods.[40] The information derived from the rheological measurements is of great importance for disclosing the delicate influences of added CNTs and shear flow on the crystallization kinetics as will be presented in this paper.

In this work, the CNT/iPP nanocomposites with relatively homogeneous dispersion of CNTs in the iPP matrix were prepared. The chemical modification of CNTs of large aspect ratio was applied before the preparation of CNT/iPP nanocomposites.[45] Differential scanning calorimetry (DSC) was used to study the quiescent crystallization kinetics of these nanocomposites with different CNT contents. The morphological evolutions and crystallization kinetics of CNT/iPP nanocomposite were investigated by using polarized optical microscopy (POM) equipped with a Linkam optical shearing system and rotational rheometer, respectively. The degree of space filling, crystallization half-time, and nucleation density (too high to be measured by optical microscope method) were quantified from the rheological measurements to shed light on the synergetic effect of added CNTs and shear flow on crystallization kinetics of CNT/iPP nanocomposites.

EXPERIMENTAL SECTION

Materials. The isotactic polypropylene used in this study was purchased from the Aldrich company, which has weight-average molecular mass of 392 kg/mol, polydispersity index of 5.8, and a melt flow index (MFI, 230 °C, 21.6 kg) of 4 g/10 min. The aligned carbon nanotubes (CNTs, model Flo Tube 7000) possess diameters of ∼6−8 nm, lengths up to ∼50 μm, and purity of above 93%. Other chemicals including xylene, chloroform, etc. were purchased from Sinopharm Chemical Reagent Co., Ltd., China and were used as received.

Sample Preparation. Before preparation of CNT/iPP nanocomposites the pristine CNTs were chemically modified to obtain modified CNTs, CNT$(COOC_{18}H_{37})_n$ by a grafting reaction with 1-bromooctadecane according to the method suggested by Qin et al.[45] CNT/iPP nanocomposites with predetermined contents of modified CNTs were prepared by solution blending. The detailed procedure is described as follows. The iPP granules were dissolved in xylene (iPP concentration of 3 wt %) at 130 °C under protection of nitrogen atmosphere in an oil bath for 30 min, followed with stirring at 120 °C for 1 h to form solution. The modified CNTs xylene suspension (CNT concentration of 0.25 wt %) treated with ultrasonication was added into the prepared iPP xylene solution. The mixture was further stirred for another 1 h before precipitation into excess cold methanol. The precipitated nanocomposite was washed with methanol three times and filtrated. Finally, the nanocomposite was dried at ambient temperature for 48 h and further dried under vacuum at 60 °C for 72 h. Six CNT/iPP nanocomposite samples having modified CNT content of 0, 0.02, 0.05, 0.1, 0.5, and 1.0 wt %, respectively, were prepared by using the above procedure.[46]

Thermogravimetric Analysis. Thermogravimetric analysis (TGA) measurements on pristine CNTs and modified CNTs, CNT$(COOC_{18}H_{37})_n$ were carried out on a TA Q5000IR thermogravimetric analyzer (TA Instruments). The samples were kept at 100 °C for 30 min under nitrogen atmosphere to erase any absorbed oxygen and water vapor. Then the samples were heated from 50 to 700 °C at a heating rate of 10 °C/min. The mass percentage of the alkyl chains grafted on the CNTs was estimated to be ∼20% from the obtained TGA curves.

Morphological Observation by Transmission Electron Microscopy. The structure and morphology of modified CNTs, CNT$(COOC_{18}H_{37})_n$ were characterized by transmission electron microscopy (TEM, JEOL JEM-2010). Dilute suspension of modified CNTs in xylene was dropped onto copper grids, which were then subjected to TEM observation after xylene was evaporated.

DOI: 10.1021/am507938s
ACS Appl. Mater. Interfaces 2015, 7, 1364−1375

Rheological Measurements. Disk-shape samples of CNT/iPP nanocomposites with thickness of 1 mm and diameter of 25 mm used for rheological measurements were prepared by compression molding at 180 °C for 3 min. The rheometer (AR2000EX, TA Instruments) with a geometry diameter of 25 mm was used to measure the rheological properties of these samples at 200 °C. Dynamic frequency sweep measurements from 500 to 0.05 rad/s were carried out in the linear viscoelastic regime after erasing the sample thermal histories.

The shear-induced crystallization kinetics for CNT/iPP nanocomposites were measured by using the rheometer according to the following procedure. Each sample was held at 200 °C for 10 min to erase thermal history, and then the sample was cooled to the desired crystallization temperature of 142 °C at a cooling rate of 8 °C/min. Subsequently, preshearing and time-sweeping tests were performed. For the isothermal crystallization process a time sweep with an angular frequency of 1 rad/s and a strain of 0.2% was performed to trace the evolution of storage modulus of the sample with time until the crystallization process was completed. The gap of the parallel plates in the rheometer was automatically adjusted throughout the crystallization process to ensure the normal stress change within ±0.1 N for accuracy of the tests. The schematic indication of the thermal and shear applications as above-described can be found in our previous publication.[42] Note that the desired crystallization temperature of 142 °C was selected because the crystallization behaviors measured at this temperature could provide effective evidence to disclose the synergetic effect of added CNTs and shear flow.

Differential Scanning Calorimetry Measurements. The crystallization behaviors during a cooling process and quiescent isothermal crystallization behaviors at different temperatures for CNT/iPP nanocomposites were investigated by using a differential scanning calorimeter (DSC TA-Q2000, TA Instruments). Each sample was heated from 50 to 200 °C at a heating rate of 50 °C/min and held for 5 min to erase thermal history. For the crystallization behaviors during a cooling process, a cooling rate of 10 °C/min was applied. For the quiescent isothermal crystallization, the sample was cooled to the selected crystallization temperature at a cooling rate of 50 °C/min and held for completion of the isothermal crystallization. The selected isothermal crystallization temperatures were 134, 138, and 142 °C, respectively.

Polarized Optical Microscopy Observation. A polarized optical microscope (POM, Olympus BX51) equipped with a Linkam optical shearing system (Linkam CSS-450, Linkam Scientific Instruments) was used to trace the crystalline morphologies both at the quiescent and shear conditions. The procedure is described as follows. The gap between the two quartz windows of the shear stage was set at 10 μm. Each sample was melted at 200 °C for 5 min to eliminate thermal history and then cooled to the crystallization temperature of 142 °C at a cooling rate of 30 °C/min. Once the crystallization temperature reached 142 °C, a steady shear with certain shear rate $\dot{\gamma}$ and shear time t_s was applied, and then the polarized optical micrographs were taken immediately after the shear cessation to record the evolution of crystalline morphology. The appropriate shear conditions were selected as follows: $\dot{\gamma}$ = 5 s^{-1}, t_s = 5 s; $\dot{\gamma}$ = 5 s^{-1}, t_s = 10 s; and $\dot{\gamma}$ = 10 s^{-1}, t_s = 5 s. We notice here that the above shear conditions were also applied in the rheological measurements for comparison purposes.

RESULTS AND DISCUSSION

Dispersion of Modified CNTs in CNT/iPP Nanocomposites. Figure 1 shows TEM micrographs of the chemically modified CNTs. The modified CNTs show loose and disentangled morphology as shown in Figure 1a, which indicates a favorable dispersion of the modified CNTs in xylene. Some defects on CNT surfaces as pointed out by the blue arrows can be seen in Figure 1b due to the surface modification through grafting of the alkyl chains. The modified CNTs can be well-dispersed in xylene, and the grafted alkyl chains increase the compatibility between dispersed CNTs and iPP matrix, both of which benefit the fine dispersion of CNTs in the CNT/iPP nanocomposites. Figure 2 shows the phase contrast optical micrographs of CNT/iPP nanocomposites with various CNT contents. These optical micrographs demonstrate that the modified CNTs are relatively uniformly dispersed in the iPP matrix at least at the micrometer scale. Only distinct large CNT aggregates can be seen at the highest CNT content of 1.0 wt % as indicated in Figure 2f. We note here the sufficient dispersion of CNTs is assisted by chemical modification of CNTs, which cannot be accomplished by using pristine CNTs as confirmed in our previous work.[47] Nevertheless, the dispersion of CNTs with content of 1.0 wt % is less satisfactory as compared to the method adopted by Vega and Trujillo et al.,[26−29] in which CNT/polyethylene (CNT/PE) nanocomposites were prepared by melt mixing PE with in situ polymerized PE-CNT masterbatch, mainly due to the much shorter alkyl chains grafted on the CNTs and the high aspect ratio of the CNTs used in the present work.

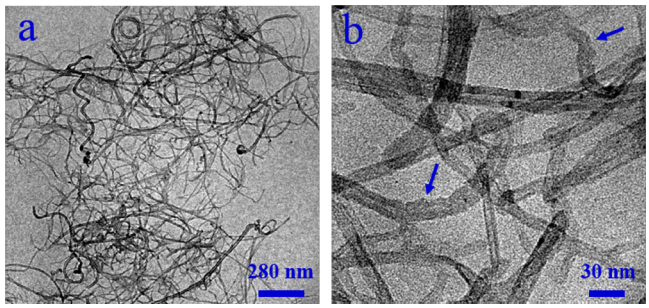

Figure 1. TEM micrographs of the modified CNTs dispersed in xylene at (a) low and (b) high magnifications.

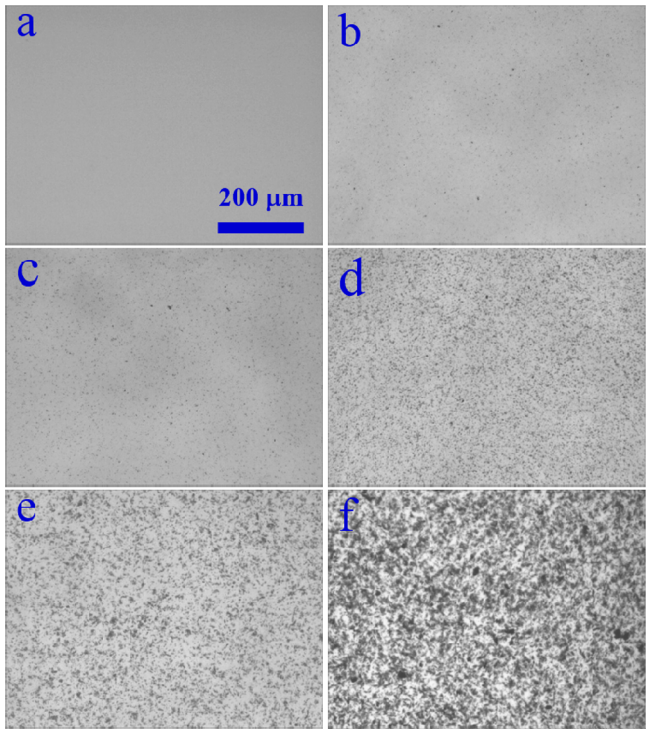

Figure 2. Phase contrast optical micrographs of neat iPP (a) and CNT/iPP nanocomposites with CNT contents of (b) 0.02, (c) 0.05, (d) 0.1, (e) 0.5, and (f) 1.0 wt %. The samples were observed in the molten state at 200 °C.

DOI: 10.1021/am507938s
ACS Appl. Mater. Interfaces 2015, 7, 1364−1375

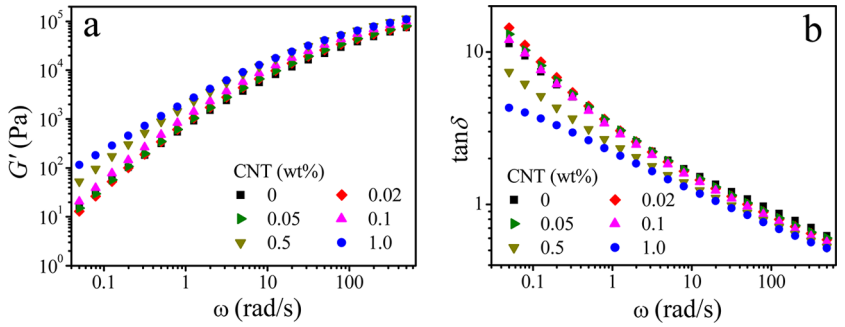

Figure 3. Changes of (a) storage modulus G' and (b) loss tangent tan δ as functions of angular frequency ω at 200 °C for CNT/iPP nanocomposites with different CNT contents.

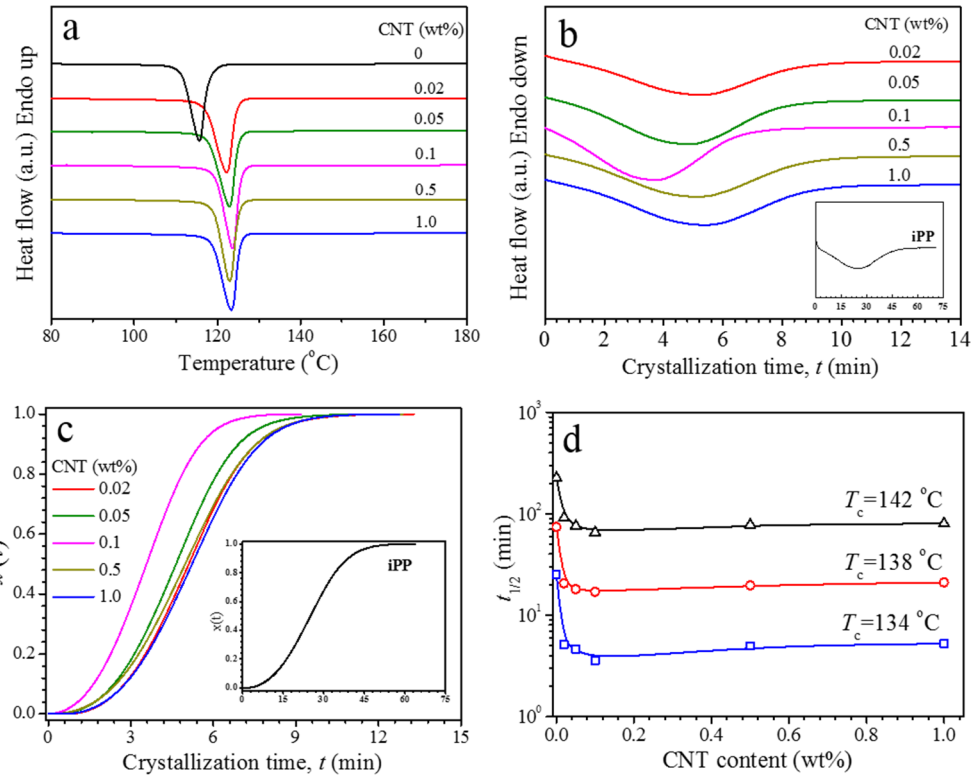

Figure 4. (a) DSC heat flow curves during cooling at a cooling rate of 10 °C/min for neat iPP and CNT/iPP nanocomposites. (b) DSC heat flow curves and (c) changes of relative crystallinity, $x(t)$ as functions of crystallization time during isothermal crystallization at 134 °C for neat iPP (inset) and CNT/iPP nanocomposites. The heat flow curves are shifted vertically to avoid overlap for clarity. (d) Changes of crystallization half-time $t_{1/2}$ as functions of CNT content for neat iPP and CNT/iPP nanocomposites under quiescent isothermal crystallization at different temperatures.

Relaxation Behaviors of CNT/iPP Nanocomposites. The changes of storage modulus G' and loss tangent tan δ as functions of angular frequency ω at 200 °C for CNT/iPP nanocomposites with different CNT contents are shown in Figure 3. The addition of CNTs with contents below 0.1 wt % brings no remarkable changes to the dependences of G' and tan δ on ω at low frequencies. As the CNT content reaches 0.5 wt % or above, the dependences of G' and tan δ on ω at low frequencies become less obvious, suggesting that the relaxation behavior becomes slower, which can be ascribed to the restrained long-range motions of macromolecular chains due to the addition of CNTs. It has been reported that there exists a "rheological percolation threshold" at which the change of tan δ at low frequencies is independent of ω. At sufficiently high CNT contents close to the rheological percolation threshold,[25,48,49] the CNT networks form and restrain the long-range motion of macromolecular chains, resulting in the liquid-like to solid-like phase transition. The rheological behaviors for CNT/iPP nanocomposites shown in Figure 3 remain similar, and the frequency-independence of tan δ at low frequencies is not observed, demonstrating that the rheological percolation threshold has not been approached in this study. Different values of percolation threshold can be found in the literature for several types of CNT/polymer nanocomposites depending on the dispersion state, the aspect ratio of CNTs, and the interactions between CNTs and the polymer matrix.[48] The absence of CNT networks in CNT/iPP nanocomposites in this study avoids the complexities resulting from the deformation of CNT networks, which makes the shear-induced crystallization results more understandable.

Quiescent Crystallization Behaviors for CNT/iPP Nanocomposites. The quiescent crystallization behaviors

DOI: 10.1021/am507938s
ACS Appl. Mater. Interfaces 2015, 7, 1364−1375

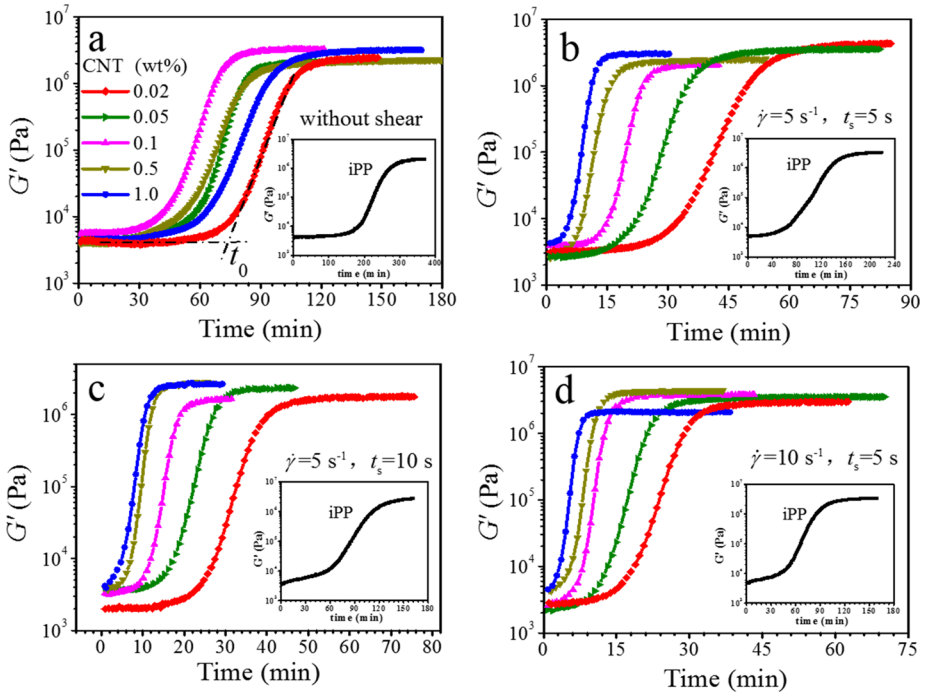

Figure 5. Changes of storage modulus, G', with crystallization time for neat iPP (inset) and CNT/iPP nanocomposites with different CNT contents during isothermal crystallization at T_c of 142 °C under the quiescent condition (a) and different shear conditions of (b) $\dot{\gamma}$ = 5 s^{-1}, t_s = 5 s; (c) $\dot{\gamma}$ = 5 s^{-1}, t_s = 10 s, and (d) $\dot{\gamma}$ = 10 s^{-1}, t_s = 5 s.

without any application of shear flow for CNT/iPP nanocomposites were studied at first for comparison purposes. Figure 4a shows the DSC heat flow curves for neat iPP and CNT/iPP nanocomposites during cooling at a cooling rate of 10 °C/min. It can be seen that the added CNTs of a low content of 0.02 wt % can induce iPP crystallization at higher temperature than neat iPP, indicating that the addition of CNTs apparently accelerates crystallization of iPP due to strong heterogeneous nucleation effect of CNTs in the composites.[46] Further increases of CNT content lead to a slight enhancement of iPP crystallization, and slight reductions of crystallization eventually occur when the CNT content increases to 0.5 and 1.0 wt %. Figure 4b,c shows the DSC heat flow curves and evolutions of the relative crystallinity, $x(t)$ for CNT/iPP nanocomposites with different CNT contents during isothermal crystallization at 134 °C. The result shows that the time to accomplish the primary crystallization reduces from ~60 min for neat iPP to 9 min for 0.02 wt % CNT/iPP nanocomposite, indicating a significant enhancement of crystallization rate due to addition of CNTs.[50] When the CNT content increases from 0.02 to 0.1 wt %, further enhancements of crystallization rate are obvious. However, when the CNT content increases to 0.5 wt % or above, the crystallization rate decreases, becoming close to that for 0.02 wt % CNT/iPP nanocomposite.

Figure 4d further shows the changes of crystallization half-time $t_{1/2}$ as functions of CNT content for CNT/iPP nanocomposites under quiescent isothermal crystallization at different temperatures. The crystallization half-time $t_{1/2}$ can be extracted to characterize the crystallization rate from the DSC measurements.[51] The acceleration effect of added CNTs on crystallization rate is prominent with CNT content of 0.02 wt %, becomes saturated when the CNT content reaches 0.1 wt %, and is slightly weakened with further increases of CNT content. The above results indicate a critical CNT content C_s* of 0.1 wt % for CNT/iPP nanocomposites, above which the acceleration effect of added CNTs on crystallization rate is saturated or even hindered. A similar critical CNT content of 0.1 wt % can be found, above which sparse aggregates of CNTs begin to form (Figure 2d), implying that the formation of CNT aggregates is related to the saturation effect of the added CNTs on crystallization rate. The addition of CNTs shows two types of effects on the crystallization behavior of iPP. On one hand, CNTs act as heterogeneous nucleating agent to increase the nucleation rate, leading to an increase of the overall crystallization rate. On the other hand, the addition of CNTs of higher content can induce topological confinement effects that can eventually result in a reduction in nucleation and crystallization kinetics.[26,28,29,36,39,46] In addition, the formation of CNT aggregates at high CNT contents as above-mentioned decreases the nucleating efficiency of individual CNTs, also contributing to the reduction of crystallization kinetics.[36] The critical CNT content of 0.1 wt % in this study is much lower than that reported in our previous work (3.8 wt %), which can be attributed to the much higher aspect ratio of the CNTs used in this study.[52−54]

Shear-Induced Isothermal Crystallization Kinetics for CNT/iPP Nanocomposites. Rheological method has been widely used to study the shear-induced crystallization of iPP because this experimental technique can provide the shear flow on the samples and then measure the rheological parameter changes of the samples during crystallization.[40,55−57] The increase of the storage modulus, G', measured by the rheological method can be correlated to the growth of crystals by modeling the crystallizing material as a suspension with filler particles (analogue to crystals) embedded in the amorphous polymer matrix. Figure 5 shows the changes of G' with crystallization time at T_c of 142 °C for CNT/iPP nanocomposites with different CNT contents under the quiescent and shear conditions. In general, the changes of G' with

DOI: 10.1021/am507938s
ACS Appl. Mater. Interfaces 2015, 7, 1364−1375

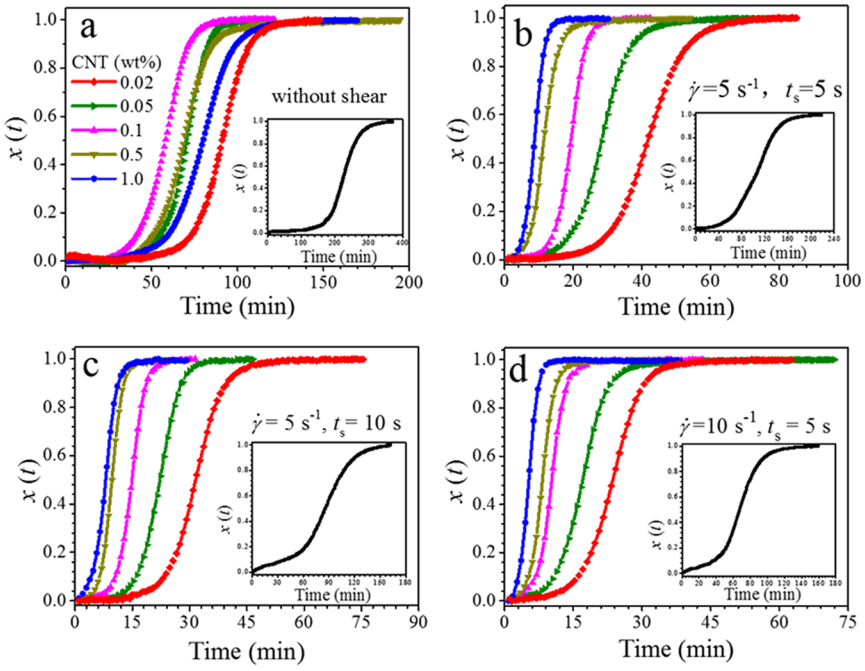

Figure 6. Changes of relative crystallinity, $x(t)$, with crystallization time for neat iPP (inset) and CNT/iPP nanocomposites with different CNT contents during isothermal crystallization at T_c of 142 °C under the quiescent condition (a) and different shear conditions of (b) $\dot{\gamma}$ = 5 s^{-1}, t_s = 5 s; (c) $\dot{\gamma}$ = 5 s^{-1}, t_s = 10 s, and (d) $\dot{\gamma}$ = 10 s^{-1}, t_s = 5 s.

crystallization time show sigmoidal shapes during the isothermal crystallization process, indicating an evolution of G' from the initial low plateau value before the beginning of crystallization to a rapid increase, and then approaching the later high plateau value at the ending of the primary crystallization stage.[50,58,59] The onset time for the rapid increase of G' is often defined as the induction time, t_0, for nucleation (illustrated by the crossover point of two dash-dot lines in Figure 5a), reflecting the energy barrier for crystallization kinetics.[59] For the quiescent condition shown in Figure 5a, t_0 is greatly reduced to ∼70 min when the CNT content is 0.02 wt %, compared with t_0 of ∼200 min for neat iPP. The t_0 reaches a minimum value at the CNT content of 0.1 wt % and then starts to increase with further increasing CNT content, implying that the acceleration effect of added CNTs on nucleation at the quiescent condition becomes deteriorated when CNT content is above 0.1 wt %. On the contrary, for CNT/iPP nanocomposites under the shear conditions as shown in Figures 5b–d, the induction time t_0 keeps decreasing with increasing CNT content in each of the three applied shear conditions, which means that the saturation effect of the added CNTs of above a critical value, C_s*, on the crystallization kinetics at the quiescent condition can be removed by application of shear flow. Note that the variations of G' in the plateau region at the end of the primary crystallization stage are probably due to the sample thickness differences coming from the fluctuations of gap distance and the sample position differences in between the parallel plates of the rheometer.

Figure 6 further shows the changes of relative crystallinity $x(t)$ with crystallization time for CNT/iPP nanocomposites with different CNT contents under the quiescent and shear conditions at T_c of 142 °C. The relative crystallinity can be estimated by logarithmically normalizing G', following the method proposed by Pogodina et al.[60] as follows:

$$x(t) = \frac{\log G'(t) - \log G'_{min}}{\log G'_{max} - \log G'_{min}} \quad (1)$$

where G'_{min} and G'_{max} are the values of the initial storage modulus and ending plateau storage modulus, respectively. By defining the crystallization half-time, $t_{1/2}$, at which the relative crystallinity reaches the value of 0.5, the influences of CNTs on the crystallization kinetics of CNT/iPP nanocomposites under the quiescent and shear conditions can be quantified. Figure 7

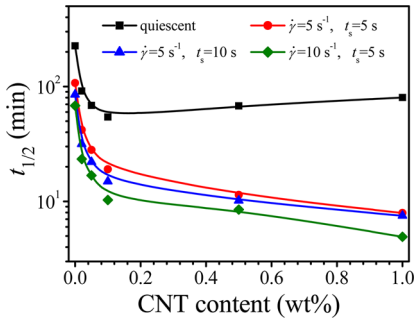

Figure 7. Changes of crystallization half-time, $t_{1/2}$, with CNT content for CNT/iPP nanocomposites isothermally crystallized at T_c of 142 °C under the quiescent and different shear conditions.

shows the changes of crystallization half-time, $t_{1/2}$, with CNT content for CNT/iPP nanocomposites isothermally crystallized at T_c of 142 °C under the quiescent and different shear conditions. It can be seen that under the quiescent condition the crystallization kinetics is dramatically accelerated when CNT content is increased to 0.1 wt %, indicated by the rapid decease of $t_{1/2}$. However, further increase of CNT content results in a slight increase in $t_{1/2}$, suggesting that the acceleration effect of CNTs on the crystallization kinetics is saturated when CNT content reaches above 1.0 wt %. The

DOI: 10.1021/am507938s
ACS Appl. Mater. Interfaces 2015, 7, 1364–1375

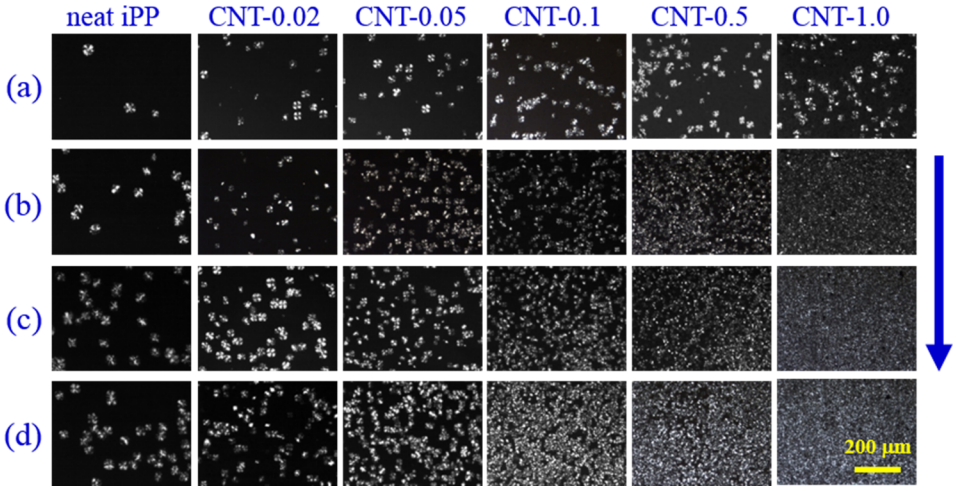

Figure 8. Selected POM micrographs for CNT/iPP nanocomposites with different CNT contents during isothermal crystallization at T_c of 142 °C under the quiescent condition (a) and different shear conditions of (b) $\dot{\gamma} = 5\ s^{-1}$, $t_s = 5$ s; (c) $\dot{\gamma} = 5\ s^{-1}$, $t_s = 10$ s, and (d) $\dot{\gamma} = 10\ s^{-1}$, $t_s = 5$ s. The scale bar in the bottom right micrograph represents 200 μm and is applied to all other micrographs. The arrow on the right side of the figure indicates the shear flow direction.

result from the rheological measurements coincides well with that obtained by DSC measurement (Figure 4d), whereas when shear flow is applied, the effects of added CNTs on the crystallization kinetics for CNT/iPP nanocomposites are much different from those under the quiescent condition. First, much more significant decrease in $t_{1/2}$ occurs when CNT content is increased to 0.1 wt % as compared to that under the quiescent condition. Second, when the CNT contents are above 0.1 wt %, $t_{1/2}$ keeps decreasing with increasing CNT content under the shear conditions, suggesting continuous acceleration of the crystallization kinetics with no saturation effect that exists under the quiescent condition. These results demonstrate that shear flow for CNT/iPP nanocomposites not only eliminates the saturation effect of CNTs on crystallization kinetics existing under the quiescent condition but also leads to a continuous acceleration effect of CNTs, even at above the critical CNT content C_s*. The greatly accelerated crystallization kinetics for CNT/iPP nanocomposites can mostly be attributed to the increase of nucleation density because the orientation of macromolecular chains and the formation of primary nuclei for CNT/iPP nanocomposites under the shear conditions become much easier than that under the quiescent conditions.[61,62] It can be further seen from Figure 7 that increasing shear rate is more effective than increasing shear time for enhancing the crystallization kinetics under the same shear strain, which is revealed by more obvious decreases in $t_{1/2}$ with the shear rate increased from 10 to 5 s^{-1} and a constant shear time of 5 s than with the shear time increased from 5 to 10 s and a constant shear rate of 5 s^{-1}, because a higher shear rate can make the macromolecular chains more highly stretched and aligned on the surfaces of CNTs.[10,62]

Morphological Evolution for CNT/iPP Nanocomposites under Various Shear Conditions. The morphological evolutions for CNT/iPP nanocomposites with different CNT contents during crystallization under the quiescent and shear conditions at 142 °C are shown in Figure 8. These polarized optical micrographs indicate that only spherulites are formed under the chosen shear conditions, and the absence of observable orientated crystals or shish-kebabs suggests that the applied shear intensity in this study is insufficient to induce strong orientation of the macromolecular chains. Improving the shear rate and/or shear time and the content of CNTs merely leads to the variations of nucleation density and scale of spherulites. Therefore, the differences in the number of nuclei (point-like nuclei) in Figure 8 deserve a detailed analysis to probe how shear flow and CNTs influence the nucleation process. In the quiescent crystallization process, the nucleation density is improved with increasing CNT content (Figure 8a). However, obvious change in nucleation density is not found with further increasing CNT content from 0.1 to 0.5 wt %, indicating the saturation effect of CNTs on the crystallization kinetics for CNT/iPP nanocomposties under the quiescent condition, in agreement with the DSC and rheological results. It can be seen from Figure 8b that the nucleation density is continuously improved with increasing CNT content under the shear condition with a shear rate of 5 s^{-1} and shear time of 5 s. Moreover, the enhancement of nucleation density becomes more significant when the CNT content increases from 0.1 to 0.5 wt %. The similar phenomenon can be seen for the shear conditions with a shear rate of 5 s^{-1} and shear time of 10 s (Figure 8c) and with a shear rate of 10 s^{-1} and shear time of 5 s (Figure 8d), for which the enhancements of nucleation density with increasing shear rate or shear time can be also concluded. Note that the spherulites in individual micrographs in Figure 8 possess about the same dimensions, indicating that these spherulites grow from the nuclei, which nucleate simultaneously after the shear flow. Overall, the enhancements of nucleation density observed by POM can be well-correlated to the acceleration of crystallization kinetics analyzed by the quantification of the crystallization half-time, $t_{1/2}$, by using the rheological method (Figure 7), and the sufficient consistency suggests that the enhancements of nucleation density by added CNTs combined with shear flow contribute greatly to the acceleration of crystallization kinetics for CNT/iPP nanocomposties.

Determination of Nucleation Densities for CNT/iPP Nanocomposites under Quiescent and Shear Conditions. It has been demonstrated that added CNTs and shear flow can greatly accelerate the crystallization kinetics for CNT/iPP nanocomposites. Polarized optical micrographs in Figure 8 further indicate that the acceleration effect is achieved by the enhancement of nucleation density for CNT/iPP nano-

DOI: 10.1021/am507938s
ACS Appl. Mater. Interfaces 2015, 7, 1364−1375

composites under the shear conditions. Therefore, it is necessary to quantify the nucleation density enhancements induced by the combined effects of added CNTs and shear flow, which can be obtained from the rheological data.

By modeling the crystallizing polymer as a suspension of growing particles in an amorphous polymer matrix, the increase of storage modulus, G', during the crystallization process can be attributed to the space-filling effect of crystals. The Kolmogorov–Avrami–Evans formula (eq 2)[63−65] was usually adopted to describe the space-filling effect of growing spherulites during the quiescent isothermal crystallization process:

$$\phi(t) = 1 - \exp\left[-\frac{3}{4}\pi N G(t)^3 (t - t_0)^3\right] \quad (2)$$

where $\phi(t)$ is the degree of space-filling, N is the nucleation density, and $G(t)$ is the spherulitic growth rate. If the nucleation and crystal growth occur during shear flow, both the nucleation density and crystal growth rate can be influenced by shear flow. In our case, most of the nucleation takes place during shear flow, and crystal growth occurs after the shear flow cessation. Furthermore, the crystalline morphology remains spherulitic with no phase transition to a shish-kebab morphology. The results from POM suggest that all the crystals form simultaneously. Therefore, it is acceptable to determine the nucleation density by applying the Kolmogorov–Avrami–Evans formula. To examine if the spherulitic growth rate is unaltered by either added CNTs or shear flow, the changes of spherulite radius with crystallization time for neat iPP and 0.05 wt % CNT/iPP nanocomposite under the quiescent and shear conditions at T_c of 142 °C are shown in Figure 9. It can be seen that all spherulitic radii change linearly

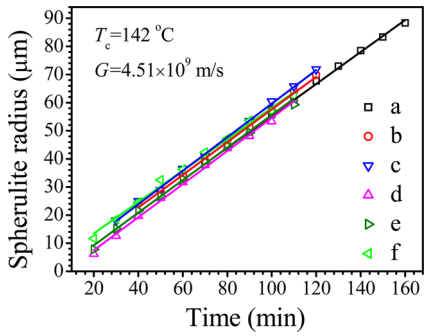

Figure 9. Change of spherulite radius as a function of time during isothermal crystallization at T_c of 142 °C under the quiescent condition for (a) neat iPP and (b) 0.05 wt % CNT/iPP nanocomposite, under the shear condition of 5 s^{-1} for 5 s for (c) neat iPP and (d) 0.05 wt % CNT/iPP nanocomposite, and under the shear condition of 5 s^{-1} for 10 s for (e) neat iPP and (f) 0.05 wt % CNT/iPP nanocomposite.

with time for neat iPP and 0.05 wt % CNT/iPP nanocomposite and that the linearly fitted lines with the same slope provide a constant spherulitic growth rate G of 4.51 × 10^{-9} m/s, which illustrates that the shear flow in this study does not influence the spherulitic growth rates, because the spherulitic growth only occurs after the shear flow cessation.[40,42,59] The crystallization kinetics is controlled by nucleation and crystal growth. Thus, the accelerated crystallization kinetics as indicated in Figure 7 can be mostly attributed to the enhancement of nucleation density, with the spherulitic growth rate unaltered under the adopted thermal and shear protocol.

With the assumption that all the nuclei are produced after the shear flow cessation, the nucleation density, N, can be estimated from the degree of space filling, ϕ, using the Avrami equation (eq 3), taking the spherulitic growth rate G of 4.51 × 10^{-9} m/s.

$$N = \frac{-3\ln[1 - \phi(t)]}{4\pi G(t)^3 t^3} \quad (3)$$

The degree of space filling, ϕ, can be calculated by using eq 1, which can be considered as the relative crystallinity. The changes of nucleation density as functions of space filling for neat iPP and CNT/iPP nanocomposites crystallized under the quiescent and shear conditions at T_c of 142 °C are shown in Figure 10. It can be seen that the nucleation density for each curve remains almost stable between ϕ of 0.1 and 0.9. The deviations at the low and high ϕ values can be attributed to the variations of G'_{min} and G'_{max} among the experiments as suggested by Housmans et al.[40] The nucleation density can be determined in two ways: (1) taking the average value between ϕ of 0.1 and 0.9; (2) taking the value at ϕ of 0.5. Both obtained values in our case are well-comparable. Thus, we chose the values obtained by the second way as the nucleation densities N.

The changes of nucleation density determined from the suspension modeling as functions of CNT content for CNT/iPP nanocomposites crystallized under the quiescent and shear conditions at T_c of 142 °C are shown in Figure 11. It can be found that added CNTs with contents of 0.1 wt % or above lead to the saturation effect on nucleation, and eventually a slight decrease in nucleation density occurs as the CNT content further increases under the quiescent condition. The nucleation density is promoted by a factor of 1 order of magnitude as the CNT content increases from 0 to 1.0 wt % under the quiescent condition. The significant finding is that once the shear flow with a shear rate of 5 s^{-1} and shear time of 5 s is applied for CNT/iPP nanocomposites, the nucleation density keeps increasing even when the CNT content exceeds 0.1 wt %, and the saturation effect appearing under the quiescent condition does not exist under the shear condition. Under the shear condition, the nucleation density is improved by a factor of 3 orders of magnitude when the CNT content is increased to 1.0 wt %. Moreover, when the shear time is increased from 5 to 10 s for the shear rate of 5 s^{-1}, further increase in nucleation density emerges. When the shear rate is improved from 5 to 10 s^{-1} for the shear time of 5 s, the enhancement of nucleation density is more remarkable, suggesting that increasing shear rate is more efficient than increasing shear time for promoting nucleation. Because added CNTs and shear flow can both enhance the nucleation density for CNT/iPP nanocomposites, one would speculate that the greatly enhanced nucleation density results from the CNT-induced heterogeneous nucleation and shear-induced nucleation, that is, an additive effect of added CNTs and shear flow, which can be expressed by eq 4:

$$N = N_c + N_s \quad (4)$$

where N_c is the CNT-induced heterogeneous nucleation density, and N_s is the shear-induced nucleation density. However, Figure 11 shows that the differences between the nucleation density under the shear conditions and quiescent conditions are gradually enlarged with increasing CNT content, suggesting that the additive rule described by eq 4 is not

DOI: 10.1021/am507938s
ACS Appl. Mater. Interfaces 2015, 7, 1364−1375

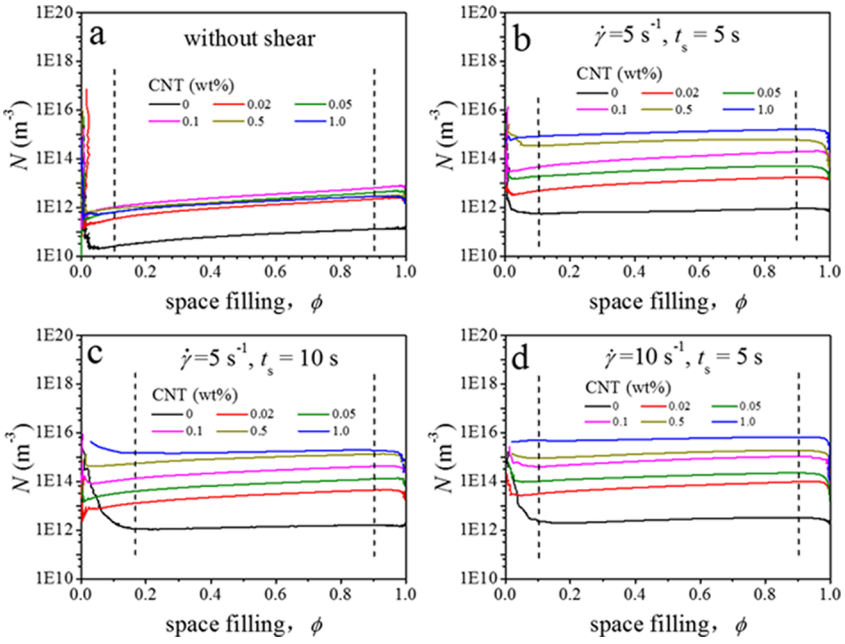

Figure 10. Changes of nucleation density, N, as functions of space filling, ϕ for CNT/iPP nanocomposites with different CNT contents during isothermal crystallization at T_c of 142 °C under the quiescent condition (a) and different shear conditions of (b) $\dot{\gamma}$ = 5 s^{-1}, t_s = 5 s; (c) $\dot{\gamma}$ = 5 s^{-1}, t_s = 10 s; and (d) $\dot{\gamma}$ = 10 s^{-1}, t_s = 5 s.

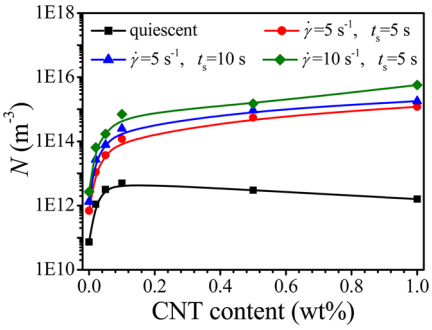

Figure 11. Change of nucleation density, N, as a function of CNT content for CNT/iPP nanocomposites during isothermal crystallization at T_c of 142 °C under the quiescent and different shear conditions.

suitable for the CNT/iPP nanocomposite system. Instead, the results can be regarded as the evidence of a synergetic rule for added CNTs and shear flow on the acceleration of crystallization kinetics for CNT/iPP nanocomposites, as mentioned in other reports.[36,39] However, the studies in those reports only mentioned the synergetic effect of added CNTs and shear flow on the overall crystallization kinetics, and the synergetic effect on the changes of nucleation density was not analyzed or quantified.

Mechanism for Synergetic Effect of CNTs and Shear Flow on Enhancement of Crystallization Kinetics. The combined acceleration effects of added CNTs and shear flow on nucleation have been reported to be synergetic rather than additive.[11,36,39,46,49,66] It has been discussed that during the quiescent isothermal crystallization, a critical CNT content, C_s*, exists, above which the effect of CNTs on crystallization kinetics can be saturated or even hindered. It is well-known that CNTs serve as heterogeneous nucleating agents for iPP crystallization. However, at high CNT loadings, topological confinement effects can be induced, which leads to the reduction in nucleation and crystallization kinetics.[26−29] Furthermore, CNTs are difficult to uniformly disperse in iPP matrix due to their poor dispersion ability, and CNTs even form relatively large aggregates at the high contents as indicated in Figure 2f. The formation of distinct large aggregates lowers the heterogeneous nucleating efficiency of individual CNTs. When shear flow is applied, the nucleation density can be greatly enhanced as compared to that under the quiescent condition. Quantification of the nucleation density demonstrates the synergetic effect of added CNTs and shear flow on the enhancement of nucleation. It is considered that a stress amplification of flow usually occurs for the particle-filled systems.[19] As elongated particles, CNTs can be oriented by shear flow, causing a more powerful variant of stress amplification. The local stresses generated around the CNTs during shear flow may be reinforced, leading to an enhanced effect of shear flow on crystallization kinetics. Another possible reinforcing effect can be attributed to the decreased chain mobility due to anchoring of macromolecular chains onto CNTs, which increases the surviving chance of the precursors for nucleation.[61,67] Furthermore, the breakup of CNT aggregates can be induced by shear flow with sufficient intensity,[36] thus reviving the heterogeneous nucleating efficiency. The interplay between added CNTs and shear flow goes by the above-mentioned effects. However, further exploration and validation on the above mechanisms for the synergetic effect of added CNTs or other particles and shear flow during shear-induced crystallization for polymer nanocomposites should be made more profoundly in near future.

CONCLUSIONS

The effects of modified carbon nanotubes (CNTs) with high aspect ratio and shear flow with different shear rates and shear time on the crystallization kinetics of CNT/isotactic polypropylene (iPP) nanocomposites were investigated by using DSC, POM, and rheometry. Under the quiescent isothermal

DOI: 10.1021/am507938s
ACS Appl. Mater. Interfaces 2015, 7, 1364−1375

crystallization condition, the addition of CNTs with low contents in iPP matrix can dramatically improve the crystallization kinetics of CNT/iPP nanocomposites, which can be attributed to the heterogeneous nucleating ability of CNTs, while a saturation effect of added CNTs exists above a critical CNT content of 0.1 wt %, which can be correlated to the increased melt viscosity and formation of CNT aggregates at the high CNT contents. When shear flow is applied to CNT/iPP nanocomposites, the saturation effect disappears, and the crystallization kinetics is continuously accelerated with increasing CNT content, shear rate, and shear time. By using a modeling between the space filling and the storage modulus of a suspension system, the nucleation density can be quantified for CNT/iPP nanocomposites under various shear conditions. The enhancement of nucleation density under the shear conditions is in good accordance with the acceleration of crystallization kinetics, for which the spherulitic growth rate is basically unaltered. A synergetic rule can be found for the combined effects of added CNTs and shear flow on the acceleration of crystallization kinetics; that is, shear flow effect can become more dominant with assistance of added CNTs. The stress amplification of shear flow in the presence of CNTs, anchoring of macromolecular chains on CNT surfaces, and the shear-induced breakup of CNT aggregates might provide explanations to the observed synergetic effect.

AUTHOR INFORMATION

Corresponding Author

*Phone: +86 0551-63607703. Fax: +86 0551-63607703. E-mail: zgwang2@ustc.edu.cn.

Notes

The authors declare no competing financial interest.

ACKNOWLEDGMENTS

Z.G.W. acknowledges the financial support from the National Basic Research Program of China with Grant No. 2012CB025901.

REFERENCES

(1) Han, Z.; Fina, A. Thermal Conductivity of Carbon Nanotubes and Their Polymer Nanocomposites: A Review. *Prog. Polym. Sci.* **2011**, *36*, 914−944.

(2) Baughman, R. H.; Zakhidov, A. A.; de Heer, W. A. Carbon Nanotubes-the Route toward Applications. *Science* **2002**, *297*, 787−792.

(3) Spitalsky, Z.; Tasis, D.; Papagelis, K.; Galiotis, C. Carbon Nanotube-Polymer Composites: Chemistry, Processing, Mechanical and Electrical Properties. *Prog. Polym. Sci.* **2010**, *35*, 357−401.

(4) Zhang, H.; Wang, Z. G.; Zhang, Z. N.; Wu, J.; Zhang, J.; He, H. S. Regenerated-Cellulose/Multiwalled-Carbon-Nanotube Composite Fibers with Enhanced Mechanical Properties Prepared with the Ionic Liquid 1-Allyl-3-Methylimidazolium Chloride. *Adv. Mater.* **2007**, *19*, 698−704.

(5) Dalton, A. B.; Collins, S.; Munoz, E.; Razal, J. M.; Ebron, V. H.; Ferraris, J. P.; Coleman, J. N.; Kim, B. G.; Baughman, R. H. Super-Tough Carbon-Nanotube Fibres. *Nature* **2003**, *423*, 703−703.

(6) Bryning, M. B.; Islam, M. F.; Kikkawa, J. M.; Yodh, A. G. Very Low Conductivity Threshold in Bulk Isotropic Single-Walled Carbon Nanotube-Epoxy Composites. *Adv. Mater.* **2005**, *17*, 1186−1191.

(7) Laird, E. D.; Li, C. Y. Structure and Morphology Control in Crystalline Polymer-Carbon Nanotube Nanocomposites. *Macromolecules* **2013**, *46*, 2877−2891.

(8) Assouline, E.; Lustiger, A.; Barber, A. H.; Cooper, C. A.; Klein, E.; Wachtel, E.; Wagner, H. D. Nucleation Ability of Multiwall Carbon Nanotubes in Polypropylene Composites. *J. Polym. Sci., Part A: Polym. Phys.* **2003**, *41*, 520−527.

(9) Coleman, J. N.; Khan, U.; Gun'ko, Y. K. Mechanical Reinforcement of Polymers Using Carbon Nanotubes. *Adv. Mater.* **2006**, *18*, 689−706.

(10) Garcia Gutierrez, M. C.; Hernandez, J. J.; Nogales, A.; Pantine, P.; Rueda, D. R.; Ezquerra, T. A. Influence of Shear on the Templated Crystallization of Poly(Butylene Terephthalate)/Single Wall Carbon Nanotube Nanocomposites. *Macromolecules* **2008**, *41*, 844−851.

(11) Mago, G.; Fisher, F. T.; Kalyon, D. M. Effects of Multiwalled Carbon Nanotubes on the Shear-Induced Crystallization Behavior of Poly(Butylene Terephthalate). *Macromolecules* **2008**, *41*, 8103−8113.

(12) Xu, J. Z.; Zhong, G. J.; Hsiao, B. S.; Fu, Q.; Li, Z. M. Low-Dimensional Carbonaceous Nanofiller Induced Polymer Crystallization. *Prog. Polym. Sci.* **2014**, *39*, 555−593.

(13) Zhuravlev, E.; Wurm, A.; Pötschke, P.; Androsch, R.; Schmelzer, J. W. P.; Schick, C. Kinetics of Nucleation and Crystallization of Poly(ε-Caprolactone)-Multiwalled Carbon Nanotube Composites. *Eur. Polym. J.* **2014**, *52*, 1−11.

(14) Marco, C.; Naffakh, M.; Gomez, M. A.; Santoro, G.; Ellis, G. The Crystallization of Polypropylene in Multiwall Carbon Nanotube-Based Composites. *Polym. Compos.* **2011**, *32*, 324−333.

(15) Cruz Delgado, V. J.; Ávila Orta, C. A.; Espinoza Martínez, A. B.; Mata Padilla, J. M.; Solis Rosales, S. G.; Jalbout, A. F.; Medellín Rodríguez, F. J.; Hsiao, B. S. Carbon Nanotube Surface-Induced Crystallization of Polyethylene Terephthalate (PET). *Polymer* **2014**, *55*, 642−650.

(16) Papageorgiou, G. Z.; Nerantzaki, M.; Grigoriadou, I.; Papageorgiou, D. G.; Chrissafis, K.; Bikiaris, D. Isotactic Polypropylene/Multi-Walled Carbon Nanotube Nanocomposites: The Effect of Modification of MWCNTs on Mechanical Properties and Melt Crystallization. *Macromol. Chem. Phys.* **2013**, *214*, 2415−2431.

(17) Yang, J. H.; Wang, C. Y.; Wang, K.; Zhang, Q.; Chen, F.; Du, R. N.; Fu, Q. Direct Formation of Nanohybrid Shish-Kebab in the Injection Molded Bar of Polyethylene/Multiwalled Carbon Nanotubes Composite. *Macromolecules* **2009**, *42*, 7016−7023.

(18) Janeschitz Kriegl, H.; Ratajski, E.; Stadlbauer, M. Flow as an Effective Promotor of Nucleation in Polymer Melts: A Quantitative Evaluation. *Rheol. Acta* **2003**, *42*, 355−364.

(19) Phillips, A. W.; Bhatia, A.; Zhu, P. W.; Edward, G. Shish Formation and Relaxation in Sheared Isotactic Polypropylene Containing Nucleating Particles. *Macromolecules* **2011**, *44*, 3517−3528.

(20) Somani, R. H.; Hsiao, B. S.; Nogales, A.; Fruitwala, H.; Srinivas, S.; Tsou, A. H. Structure Development During Shear Flow Induced Crystallization of i-PP: In Situ Wide-Angle X-Ray Diffraction Study. *Macromolecules* **2001**, *34*, 5902−5909.

(21) Li, C. Y.; Li, L. Y.; Cai, W. W.; Kodjie, S. L.; Tenneti, K. K. Nanohybrid Shish-Kebabs: Periodically Functionalized Carbon Nanotubes. *Adv. Mater.* **2005**, *17*, 1198−1202.

(22) Li, L. Y.; Li, C. Y.; Ni, C. Y. Polymer Crystallization-Driven, Periodic Patterning on Carbon Nanotubes. *J. Am. Chem. Soc.* **2006**, *128*, 1692−1699.

(23) Zhang, Y.; Song, K.; Meng, J.; Minus, M. L. Tailoring Polyacrylonitrile Interfacial Morphological Structure by Crystallization in the Presence of Single-Wall Carbon Nanotubes. *ACS Appl. Mater. Interfaces.* **2013**, *5*, 807−814.

(24) Laird, E. D.; Li, C. Y. Structure and Morphology Control in Crystalline Polymer-Carbon Nanotube Nanocomposites. *Macromolecules* **2013**, *46*, 2877−2891.

(25) Du, F.; Scogna, R. C.; Zhou, W.; Brand, S.; Fischer, J. E.; Winey, K. I. Nanotube Networks in Polymer Nanocomposites: Rheology and Electrical Conductivity. *Macromolecules* **2004**, *37*, 9048−9055.

(26) Vega, J.; Martinez Salazar, J.; Trujillo, M.; Arnal, M.; Muller, A.; Bredeau, S.; Dubois, P. Rheology, Processing, Tensile Properties, and Crystallization of Polyethylene/Carbon Nanotube Nanocomposites. *Macromolecules* **2009**, *42*, 4719−4727.

(27) Vega, J. F.; da Silva, Y.; Vicente Alique, E.; Núñez Ramírez, R.; Trujillo, M.; Arnal, M. L.; Müller, A. J.; Dubois, P.; Martínez Salazar, J.

DOI: 10.1021/am507938s
ACS Appl. Mater. Interfaces 2015, 7, 1364−1375

Influence of Chain Branching and Molecular Weight on Melt Rheology and Crystallization of Polyethylene/Carbon Nanotube Nanocomposites. *Macromolecules* **2014**, *47*, 5668−5681.
(28) Trujillo, M.; Arnal, M.; Müller, A. J.; Bredeau, S.; Bonduel, D.; Dubois, P.; Hamley, I.; Castelletto, V. Thermal Fractionation and Isothermal Crystallization of Polyethylene Nanocomposites Prepared by in Situ Polymerization. *Macromolecules* **2008**, *41*, 2087−2095.
(29) Trujillo, M.; Arnal, M.; Müller, A. J.; Laredo, E.; Bredeau, S.; Bonduel, D.; Dubois, P. Thermal and Morphological Characterization of Nanocomposites Prepared by in Situ Polymerization of High-Density Polyethylene on Carbon Nanotubes. *Macromolecules* **2007**, *40*, 6268−6276.
(30) Pukanszky, B. Interfaces and Interphases in Multicomponent Materials: Past, Present, Future. *Eur. Polym. J.* **2005**, *41*, 645−662.
(31) Zhang, B.; Chen, J. B.; Cui, J.; Zhang, H.; Ji, F. F.; Zheng, G. Q.; Heck, B.; Reiter, G.; Shen, C. Y. Effect of Shear Stress on Crystallization of Isotactic Polypropylene from a Structured Melt. *Macromolecules* **2012**, *45*, 8933−8937.
(32) Fernandez Ballester, L.; Thurman, D. W.; Zhou, W. J.; Kornfield, J. A. Effect of Long Chains on the Threshold Stresses for Flow-Induced Crystallization in iPP: Shish Kebabs Vs Sausages. *Macromolecules* **2012**, *45*, 6557−6570.
(33) Jabbarzadeh, A.; Tanner, R. I. Flow-Induced Crystallization: Unravelling the Effects of Shear Rate and Strain. *Macromolecules* **2010**, *43*, 8136−8142.
(34) Zhao, B. J.; Li, X. Y.; Huang, Y. J.; Cong, Y. H.; Ma, Z.; Shao, C. G.; An, H. N.; Yan, T. Z.; Li, L. B. Inducing Crystallization of Polymer through Stretched Network. *Macromolecules* **2009**, *42*, 1428−1432.
(35) Van der Beek, M. H. E.; Peters, G. W. M.; Meijer, H. E. H. Influence of Shear Flow on the Specific Volume and the Crystalline Morphology of Isotactic Polypropylene. *Macromolecules* **2006**, *39*, 1805−1814.
(36) D'Haese, M.; Langouche, F.; Van Puyvelde, P. On the Effect of Particle Size, Shape, Concentration, and Aggregation on the Flow-Induced Crystallization of Polymers. *Macromolecules* **2013**, *46*, 3425−3434.
(37) D'Haese, M.; Van Puyvelde, P.; Langouche, F. Effect of Particles on the Flow-Induced Crystallization of Polypropylene at Processing Speeds. *Macromolecules* **2010**, *43*, 2933−2941.
(38) Naudy, S.; David, L.; Rochas, C.; Fulchiron, R. Shear Induced Crystallization of Poly(*m*-Xylylene Adipamide) with and without Nucleating Additives. *Polymer* **2007**, *48*, 3273−3285.
(39) Chen, Y. H.; Zhong, G. J.; Lei, J.; Li, Z. M.; Hsiao, B. S. In Situ Synchrotron X-Ray Scattering Study on Isotactic Polypropylene Crystallization under the Coexistence of Shear Flow and Carbon Nanotubes. *Macromolecules* **2011**, *44*, 8080−8092.
(40) Housmans, J. W.; Steenbakkers, R. J. A.; Roozemond, P. C.; Peters, G. W. M.; Meijer, H. E. H. Saturation of Pointlike Nuclei and the Transition to Oriented Structures in Flow-Induced Crystallization of Isotactic Polypropylene. *Macromolecules* **2009**, *42*, 5728−5740.
(41) Ma, Z.; Steenbakkers, R. J. A.; Giboz, J.; Peters, G. W. M. Using Rheometry to Determine Nucleation Density in a Colored System Containing a Nucleating Agent. *Rheol. Acta* **2011**, *50*, 909−915.
(42) Zhong, Y.; Fang, H. G.; Zhang, Y. Q.; Wang, Z. K.; Yang, J. J.; Wang, Z. G. Rheologically Determined Critical Shear Rates for Shear-Induced Nucleation Rate Enhancements of Poly(Lactic Acid). *ACS Sustainable Chem. Eng.* **2013**, *1*, 663−672.
(43) van Meerveld, J.; Peters, G. W. M.; Hütter, M. Towards a Rheological Classification of Flow Induced Crystallization Experiments of Polymer Melts. *Rheol. Acta* **2004**, *44*, 119−134.
(44) Vega, J. F.; Hristova, D. G.; Peters, G. W. M. Flow-Induced Crystallization Regimes and Rheology of Isotactic Polypropylene. *J. Therm. Anal. Calorim.* **2009**, *98*, 655−666.
(45) Qin, Y. J.; Shi, J. H.; Wu, W.; Li, X. L.; Guo, Z. X.; Zhu, D. B. Concise Route to Functionalized Carbon Nanotubes. *J. Phys. Chem. B* **2003**, *107*, 12899−12901.
(46) Xu, D. H.; Wang, Z. G. Role of Multi-Wall Carbon Nanotube Network in Composites to Crystallization of Isotactic Polypropylene Matrix. *Polymer* **2008**, *49*, 330−338.
(47) Kharchenko, S. B.; Douglas, J. F.; Obrzut, J.; Grulke, E. A.; Migler, K. B. Flow-Induced Properties of Nanotube-Filled Polymer Materials. *Nat. Mater.* **2004**, *3*, 564−568.
(48) Xu, D. H.; Wang, Z. G.; Douglas, J. F. Influence of Carbon Nanotube Aspect Ratio on Normal Stress Differences in Isotactic Polypropylene Nanocomposite Melts. *Macromolecules* **2008**, *41*, 815−825.
(49) Iervolino, R.; Somma, E.; Nobile, M. R.; Chen, X. M.; Hsiao, B. S. The Role of Multi-Walled Carbon Nanotubes in Shear Enhanced Crystallization of Isotactic Poly(1-Butene). *J. Therm. Anal. Calorim.* **2009**, *98*, 611−622.
(50) Wang, Z. G.; Hsiao, B. S.; Sirota, E. B.; Agarwal, P.; Srinivas, S. Probing the Early Stages of Melt Crystallization in Polypropylene by Simultaneous Small- and Wide-Angle X-Ray Scattering and Laser Light Scattering. *Macromolecules* **2000**, *33*, 978−989.
(51) Shao, W.; Zhang, Y. Q.; Wang, Z. G.; Niu, Y. H.; Yue, R. J.; Hu, W. P. Critical Content of Ultrahigh-Molecular-Weight Polyethylene to Induce the Highest Nucleation Rate for Isotactic Polypropylene in Blends. *Ind. Eng. Chem. Res.* **2012**, *51*, 15953−15961.
(52) Xu, Z. H.; Niu, Y. H.; Wang, Z. G.; Li, H.; Yang, L.; Qiu, J.; Wang, H. Enhanced Nucleation Rate of Polylactide in Composites Assisted by Surface Acid Oxidized Carbon Nanotubes of Different Aspect Ratios. *ACS Appl. Mater. Interfaces* **2011**, *3*, 3744−3753.
(53) Zhong, Y.; Zhang, Y. Q.; Yang, J. J.; Li, W. L.; Wang, Z. G.; Xu, D. H.; Chen, S. Y.; Ding, Y. S. Exponentially Increased Nucleation Ability for Poly ($_L$-Lactide) by Adding Acid-Oxidized Multiwalled Carbon Nanotubes with Reduced Aspect Ratios. *Sci. China. Chem.* **2013**, *56*, 181−194.
(54) Li, W. L.; Zhang, Y. Q.; Yang, J. J.; Zhang, J.; Niu, Y. H.; Wang, Z. G. Thermal Annealing Induced Enhancements of Electrical Conductivities and Mechanism for Multiwalled Carbon Nanotubes Filled Poly (Ethylene-co-Hexene) Composites. *ACS Appl. Mater. Interfaces.* **2012**, *4*, 6468−6478.
(55) Boutahar, K.; Carrot, C.; Guillet, J. Crystallization of Polyolefins from Rheological Measurements Relation between the Transformed Fraction and the Dynamic Moduli. *Macromolecules* **1998**, *31*, 1921−1929.
(56) Pogodina, N. V.; Lavrenko, V. P.; Srinivas, S.; Winter, H. H. Rheology and Structure of Isotactic Polypropylene near the Gel Point: Quiescent and Shear-Induced Crystallization. *Polymer* **2001**, *42*, 9031−9043.
(57) Khanna, Y. P. Rheological Mechanism and Overview of Nucleated Crystallization Kinetics. *Macromolecules* **1993**, *26*, 3639−3643.
(58) Niu, Y. H.; Yang, L.; Wang, H.; Wang, Z. G. Criteria of Process Optimization in Binary Polymer Blends with Both Phase separation and Crystallization. *Macromolecules* **2009**, *42*, 7623−7626.
(59) Fang, H. G.; Zhang, Y. Q.; Bai, J.; Wang, Z. G. Shear-Induced Nucleation and Morphological Evolution for Bimodal Long Chain Branched Polylactide. *Macromolecules* **2013**, *46*, 6555−6565.
(60) Pogodina, N. V.; Winter, H. H.; Srinivas, S. Strain Effects on Physical Gelation of Crystallizing Isotactic Polypropylene. *J. Polym. Sci., Part A: Polym. Phys.* **1999**, *37*, 3512−3519.
(61) Xu, J. Z.; Chen, C.; Wang, Y.; Tang, H.; Li, Z. M.; Hsiao, B. S. Graphene Nanosheets and Shear Flow Induced Crystallization in Isotactic Polypropylene Nanocomposites. *Macromolecules* **2011**, *44*, 2808−2818.
(62) Tang, H.; Chen, J. B.; Wang, Y.; Xu, J. Z.; Hsiao, B. S.; Zhong, G. J.; Li, Z. M. Shear Flow and Carbon Nanotubes Synergistically Induced Nonisothermal Crystallization of Poly (Lactic Acid) and Its Application in Injection Molding. *Biomacromolecules* **2012**, *13*, 3858−3867.
(63) Avrami, M. Granulation, Phase Change, and Microstructure-Kinetics of Phase Change. III. *J. Chem. Phys.* **1941**, *9*, 177−184.
(64) Evans, U. The Laws of Expanding Circles and Spheres in Relation to the Lateral Growth of Surface Films and the Grain-Size of Metals. *Trans. Faraday Soc.* **1945**, *41*, 365−374.

DOI: 10.1021/am507938s
ACS Appl. Mater. Interfaces 2015, 7, 1364−1375

(65) Kolmogorov, A. N. On the Statistical Theory of the Crystallization of Metals. *Izv. Akad. Nauk SSSR, Ser. Mat.* **1937**, *1*, 355−359.
(66) Garcia Gutierrez, M. C.; Hernandez, J. J.; Nogales, A.; Panine, P.; Rueda, D. R.; Ezquerra, T. A. Influence of Shear on the Templated Crystallization of Poly(Butylene Terephthalate)/Single Wall Carbon Nanotube Nanocomposites. *Macromolecules* **2007**, *41*, 844−851.
(67) Patil, N.; Balzano, L.; Portale, G.; Rastogi, S. A Study on the Chain-Particle Interaction and Aspect Ratio of Nanoparticles on Structure Development of a Linear Polymer. *Macromolecules* **2010**, *43*, 6749−6759.

DOI: 10.1021/am507938s
ACS Appl. Mater. Interfaces 2015, 7, 1364−1375